Colloid Polym Sci (2006) 284: 644–653
DOI 10.1007/s00396-005-1429-8

ORIGINAL CONTRIBUTION

Galo Cárdenas
Yasna León
Yanko Moreno
Octavio Peña

Synthesis and properties of NiSn colloids using different metal ratios by CLD

Received: 21 February 2005
Accepted: 1 November 2005
Published online: 21 January 2006
© Springer-Verlag 2006

G. Cárdenas (✉) · Y. León
Departamento de Polímeros,
Facultad de Ciencias Químicas,
Edmundo Larenas 129, casilla 160-C,
Universidad de Concepción,
Concepción, Chile
e-mail: gcardena@udec.cl
Fax: +56-41-203337

Y. Moreno
Departamento de Química
Analítica e Inorgánica,
Facultad de Ciencias Químicas,
Edmundo Larenas 129, casilla 160-C,
Universidad de Concepción,
Concepción, Chile

O. Peña
Institut de Chimie de Rennes,
Universite de Rennes I,
35042 Rennes Cedex, France

Abstract Bimetallic colloidal dispersions of Ni–Sn were prepared by simultaneous co-condensation with organic solvents at 77 K using the chemical liquid deposition (CLD) method. The atoms in a 1:1, 2:1, 3:1, 1:2 and 1:3 ratios were produced by resistive heating and were reacted with 2-propanol, 2-methoxyethanol, ethanol and acetone to produce colloids. The bimetallic films and solids were obtained by evaporation under vacuum at room temperature. The colloids and solids were characterized by several studies, including the stability at room temperature, electrophoresis, ultraviolet-visible spectrophotometry, transmission electron microscopy (TEM), electron diffraction, conductivity, nergy dispersive X-ray analysis, electrophoretic measurements, thermogravimetric analysis (TGA), X-ray photoelectron spectroscopy (XPS) and magnetic properties. TEM studies show a size distribution between 6 and 14 nm, depending of the solvent and Ni:Sn ratio. We can observe a high stability for the colloidal dispersion with different solvents (>2 weeks); this is due mainly to the solvation capacity and polarity of the organic molecules. Electrophoretic measurements revealed that the particles are weakly positively charged with a greater Ni percentage. Electron diffraction analysis for the metallic colloids shows the presence of bimetallic compounds as NiSn, Ni_3Sn, Ni_3Sn_4 and tin oxides. XPS analysis was used for the study of the Ni–Sn solid composition, where it was determined that the Ni atoms could be as Ni^0 and Ni^{2+}. The bond energy difference in both species were 0.8 eV; on the other side, Sn atoms showed two peaks, the first associated with Sn^0 atoms and the second attributed to oxidized species like SnO_x. The conductivity studies showed that when the metal is changed, the electric conductivity properties change too and are associated with the particle size increasing.

Keywords Bimetallic colloids · Nanostructure · Chemical liquid deposition · Semiconductors

Introduction

The intense interest in metallic cluster to nanoscale is the result of its potential theoretical importance and applications [1, 2]. The physical properties are different from the bulk and at the same time different from the atomic state. They have intermediate electronic properties; in addition, a great fraction of their atoms are located in their surface, acquiring new optical, magnetic and electronic characteristic. Furthermore, these nanoparticles change with respect to their reactivity and catalytic properties [3–12].

The properties of the nanostructures are not only determined by the size of clusters but by the way of organization in the structure of nanoclusters wherein clusters act like separated atoms. The way nanoclusters are linked in nanostructures depends not only on the properties of

separation and the interaction inter-clusters but also on the methods of the preparation used.

For the obtention of Ni nanoparticles, several techniques have been used such as vaporization with laser [13], sonochemical technique [14] and the use of organometallic precursors (chemical reduction) in the nickel particle synthesis, which has provided an efficient route for the particle obtained to have a controllable and clean surface and, in some cases, adjustable sizes. Later on, Ely et al. described the synthesis of nanoparticles of nickel prepared by decomposition of $Ni(COD)_2$ (COD: cycloocta-1,5-diene) in CH_2Cl_2 in the presence of poly(vinylpyrrolidone)[15], in which one obtains particles with clean metallic surfaces and that have magnetic properties similar to those of bulk. This precursor [$Ni(COD)_2$] has been used for the synthesis of nanoparticles of anchored nickel to amorphous coal [16].

In this work we focused on the characterization of Ni–Sn nanoparticles synthesized by chemical liquid deposition (CLD), which already have some characterizations we reported [17].

The advantage of this technique is the nanostructural materials, which by other techniques are not possible; some of the used metals that can be prepared are Au, Pd, Cu, Ni, Pt, Co, Fe, Sn, Pr, Yb and Er monometallic dispersions and Au–Pd [18], Au–Cu [19], Zn–Cd [20], Ni–Cu [21] and Ni–Sn [17] bimetallic dispersions, among others.

Experiments

Colloid formation

A typical co-condensation was carried out using the previously reported, specially designed equipment [22, 23].

Two alumina tungsten crucibles were charged with around 19.0 mg of Ni and 18.4 mg of Sn metal in lumps, respectively. Distilled and dried solvents (e.g. ethanol, 150 ml) were placed in a ligand inlet tube and freeze–pump–thaw degassed for five cycles. The reactor was pumped to 1×10^{-4} Torr, while the crucible was warmed to red heat. The temperature in the crucible at red heat should be at the boiling point of Ni and Sn since they are heated with separate electrodes (around 2,732 and 2,270°C, respectively). A liquid-nitrogen-filled Dewar was placed around the vessel, and Ni (0.322 mmol), Sn (0.155 mmol) and ethanol (100 ml) were co-deposited over a 1.5-h period at a rate of approximately 2 ml/min. The matrix was a brown color at the end of the co-deposition. The matrix was allowed to warm slowly for 1.0 h to room temperature under vacuum by removal of the liquid nitrogen Dewar. Upon meltdown, a brown dispersion was allowed to warm for another 0.5 h to room temperature. The sol was siphoned into a flask under nitrogen. Based on the amount of metal evaporated and the amount of solvent consumed, the concentration of the alloy could be calculated.

Transmission electron microscopy (TEM)

Transmission electron micrographs were obtained with a JEOL JEM 1,200 EX II with 4 Å resolution using copper grids coated with carbon foil. A drop of the colloid was placed on a 150-mesh copper grid and allowed to dry.

Electron diffraction was also carried out. In this case, the micrographs were obtained using 120 kV, 60 cm, K: 4.209 A°. The calibration was carried out with Au film (Aldrich Chemical, 99.99%) evaporated over a copper grid. The deposition was carried out using an Edwards 5,150 Evaporator.

UV-Vis absorption

The absorption spectra of the colloids were measured at 25°C in a Spectronic Genesis 2 spectrophotometer using quartz cells. The background was set up with the proper solvent, and then each colloidal sample was examined. The kinetics of clustering was followed at room temperature by taking absorption spectra every hour for 72 h.

Electrophoresis

The electrophoresis experiments were carried out using a Burton device of 11-cm glass U-tube with a stopcock on

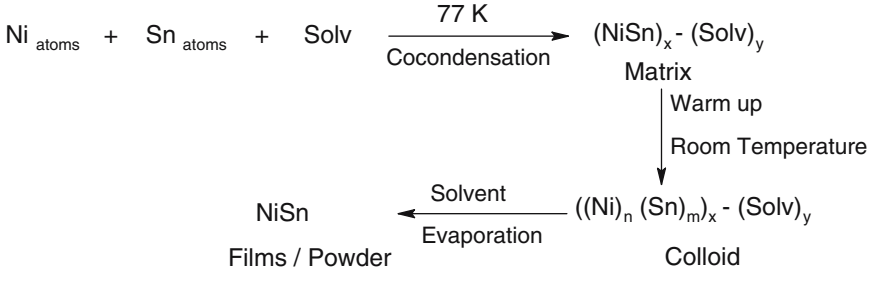

Scheme 1 Colloid and active solid formations starting from gas phase metal atoms and solvent molecules

the base to connect a perpendicular glass tube. The solvent was placed in the left side of the tube, and the colloid slowly poured on the right side. Platinum electrodes were attached to the top of the U-tube and through a ground glass joint to the pole of a power supply (200 V) [24]. A typical experiment was carried out for a 3-h period at 25°C. The column displacement was measured. To corroborate this experiment, a Zee Meter Model 501 (Pen Kem) was used.

Thermogravimetric studies

A Perkin Elmer Model TGA-7 thermogravimetric analysis (TGA) system with a microprocessor-driven temperature control unit and a TA data station was used. The mass of the samples was generally in the range 2–3 mg. The sample was placed in the balance system, and the temperature was raised from 25 to 550°C at heating rate of 10°C/min. The

Table 1 Stability and particle size of NiSn colloids

Solvent	Concentration ($\times 10^{-3}$ M)		Ni:Sn	Stability (days)	Particle size
	Ni	Sn			
2-Methoxyethanol	2.7	2.7	1:1	>30	7.8
	4.2	4.5			
2-Methoxyethanol	2.5	1.2	2:1	>30	7.5
	3.8	1.7			
2-Methoxyethanol	4.1	1.3	3:1	>30	6.7
	4.5	1.6			
2-Methoxyethanol	1.6	3.2	1:2	<30	8.4
	3.8	7.5			
2-Methoxyethanol	1.0	3.0	1:3	<30	10.5
	2.0	6.2			
2-Propanol	2.7	2.7	1:1	<15	6.9
	4.0	4.5			
2-Propanol	4.0	2.0	2:1	<15	6.9
	3.9	1.7			
2-Propanol	3.5	1.2	3:1	<15	4.5
	4.5	1.5			
2-Propanol	1.1	2.3	1:2	Coagulate	8.8
	3.8	7.4			
2-Propanol	1.5	4.0	1:3	Coagulate	11.0
	2.3	7.0			
Acetone	2.8	2.8	1:1	<2	10.4
	4.0	4.0			
Acetone	2.8	1.4	2:1	<2	8.6
	3.8	1.9			
Acetone	4.6	1.5	3:1	<2	7.2
	4.1	1.4			
Acetone	1.5	3.0	1:2	Coagulate	14.1
	3.0	6.4			
Acetone	1.5	4.8	1:3	Coagulate	14.1
	2.0	6.2			
Ethanol	3.7	3.5	1:1	>10	14.3
	–	–			
Ethanol	3.2	1.5	2:1	>10	8.6
	–	–			
Ethanol	3.7	0.61	3:1	>10	5.9
	–	–			
Ethanol	2.6	5.2	1:2	>10	15.7
	–	–			
Ethanol	2.7	8.3	1:3	>10	17.8
	–	–			

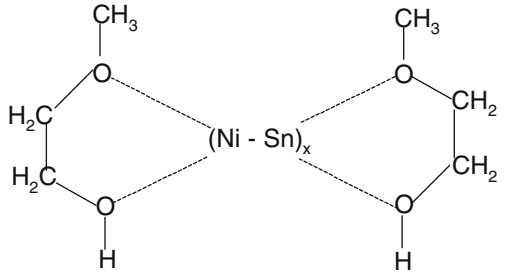

Scheme 2 Colloid bimetallic stabilization

sample weight was continuously recorded as a function of temperature.

Conductivity

The electrical conductivity measurements were carried out using 120-mg sample and making a pellet at 16,600 psi.

The electrical resistance was measured using an RCL Fluke PM 6,304 bridge, and from the area and sample thickness, the resistance was transformed to electrical resistivity, an independent parameter of the sample size.

Magnetic susceptibility

Magnetic susceptibility (SHE-VTS 906 SQUID Susceptometer) was measured between 4 and 300 K, under an applied field of 2 K Oe (0.2 T). Powder samples were placed and compacted inside a gelatin capsule. The temperature-independent magnetic contribution due to the sample holder was subtracted from all temperature measurements that were performed on a zero-field-cooled (ZFC) mode, that is, cooling the sample under zero field and then warming it under the given applied magnetic field. The diamagnetic contribution due to the core electrons was estimated using Pascal constants and subtracted from the experimental values.

Table 2 Charges and zeta potentials of NiSn colloids

Concentration ($\times10^{-3}$ M)		Ni:Sn	V ($\times10^{-6}$ m/s)	μ_E($\times10^{-9}$ m^2/Vs)	ξ (V)	Charge
Ni	Sn					
1.9	–	1:0	3.30	4.12	0.067	Positive
–	3.2	0:1	4.02	3.35	0.055	Negative
2.7	2.7	1:1	1.11	2.77	0.045	Positive
2.5	1.2	2:1	3.78	3.15	0.051	Positive
4.1	1.3	3:1	4.36	3.64	0.059	Positive
1.6	3.2	1:2	1.74	1.45	0.024	Negative
1.0	3.0	1:3	2.61	2.17	0.035	Negative

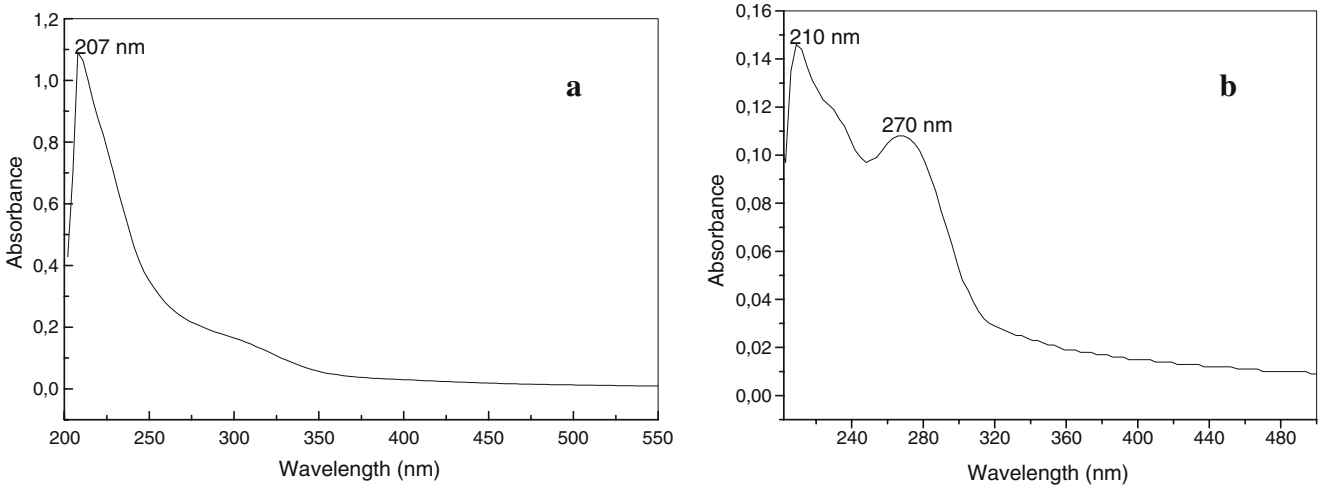

Fig. 1 **a** UV-Vis absorption spectrum of Ni:Sn (3:1) and **b** Ni:Sn (1:1) in 2-methoxyethanol

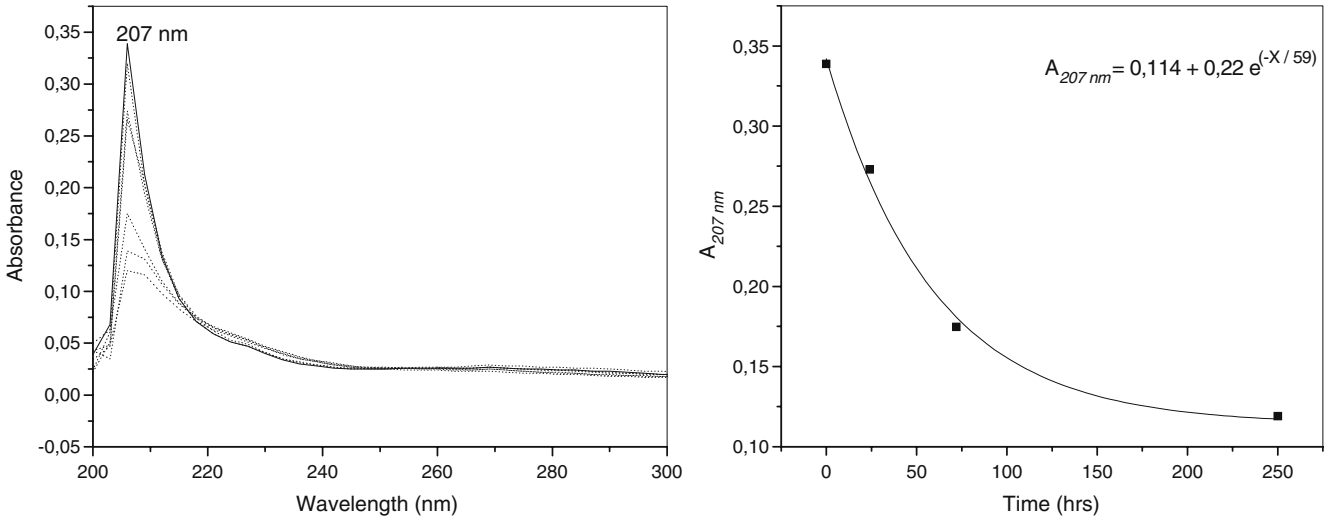

Fig. 2 UV-Vis absorption spectrum of Ni:Sn (2:1)-methoxyethanol 10^{-3} M, studied over 4 days and kinetic behavior of the 207-nm peak

X-ray photoelectron spectroscopy (XPS)

XPS spectra were recorded using a Perkin Elmer 1,257 spectrometer with a hemispherical analyzer and a monochromatized Mg Kα X-ray source (hν=1,253.6 eV) operated at 10 mA and 12 kV. The binding energy of 284.5 eV for C 1s is from surface carbon contaminant that was used for the binding energy calibration.

Results and discussion

The nickel–tin bimetallic colloids were obtained by co-condensation of the metal with several solvents, such as 2-methoxyethanol, 2-propanol, acetone and ethanol. Scheme 1 shows the synthesis of these colloids.

The stability, the metallic ratio between both metals and the concentration of the colloids are summarized in Table 1. The more stable colloids were formed in 2-methoxyethanol (>30 days). Ni–Sn bimetallic in acetone and ethanol colloids were unstable, and this is most probably due to their lower viscosity and the polarity of the dispersions. This finding is consistent with other studies previously reported [17].

The higher stability of the 2-methoxyethanol bimetallic colloid can be explained by bidentate coordination through the oxygen atoms shown in the Scheme 2.

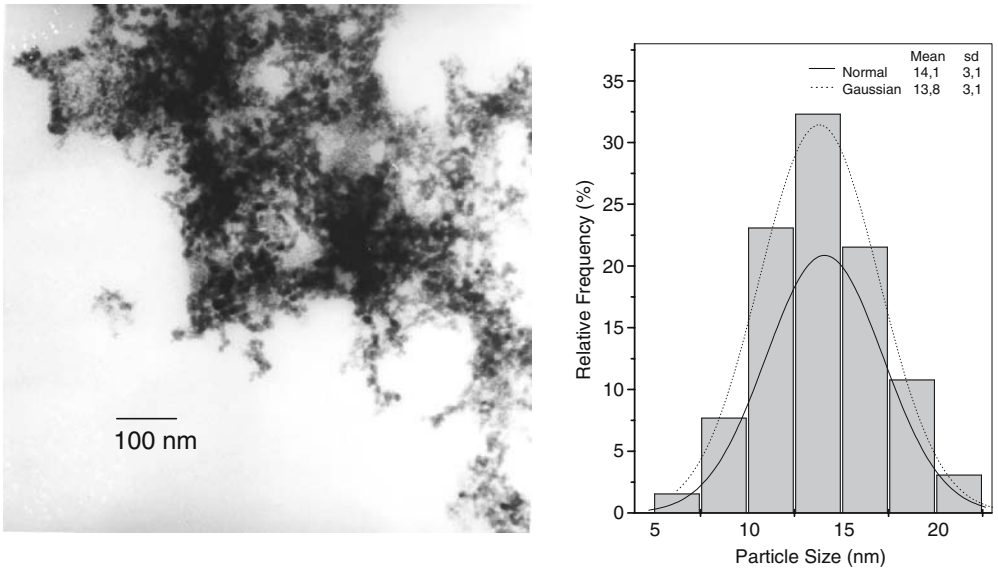

Fig. 3 Electron micrograph (100 K) and histogram of Ni–Sn–acetone (1:3) using bright field. Average particle size of Ni–Sn cluster μ=14 nm, σ=3.1 nm

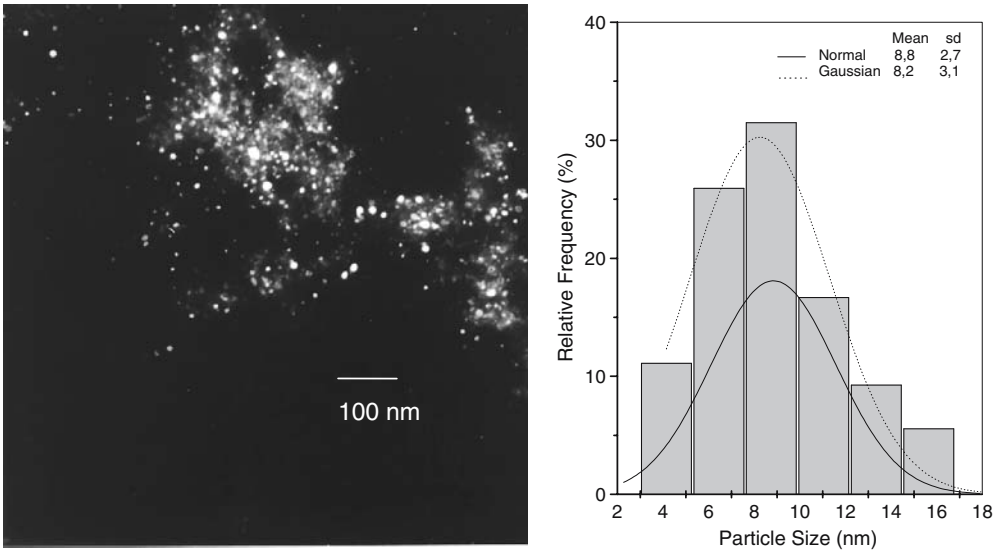

Fig. 4 Electron micrograph (100 K) and histogram of Ni–Sn–2-propanol (1:2) using dark field. Average particle size of Ni–Sn cluster μ= 8.8 nm, σ=2.7 nm

On the other hand, the particles are weakly positively or negatively charged on their surface, which can be probed by electrophoretic measurements (see Table 2).

The colloids with greater percentage of Ni migrate towards the cathode, being the positive charges, whereas the colloids with greater percentage of Sn migrates towards the anode, being the negative loads. This behavior is similar to the monometallic systems of nickel and tin previously reported [25, 26], which present positive and negative charges, respectively.

A spectroscopy study of the Ni–Sn colloids in the UV-visible region (200–800 nm) was carried out. In Fig. 1 we can see only one absorption band at 207 nm for Ni–Sn–2-methoxyethanol (3:1 ratio); as the amount of Sn (1:1 ratio) is increased, two absorption bands can be seen at 210 and

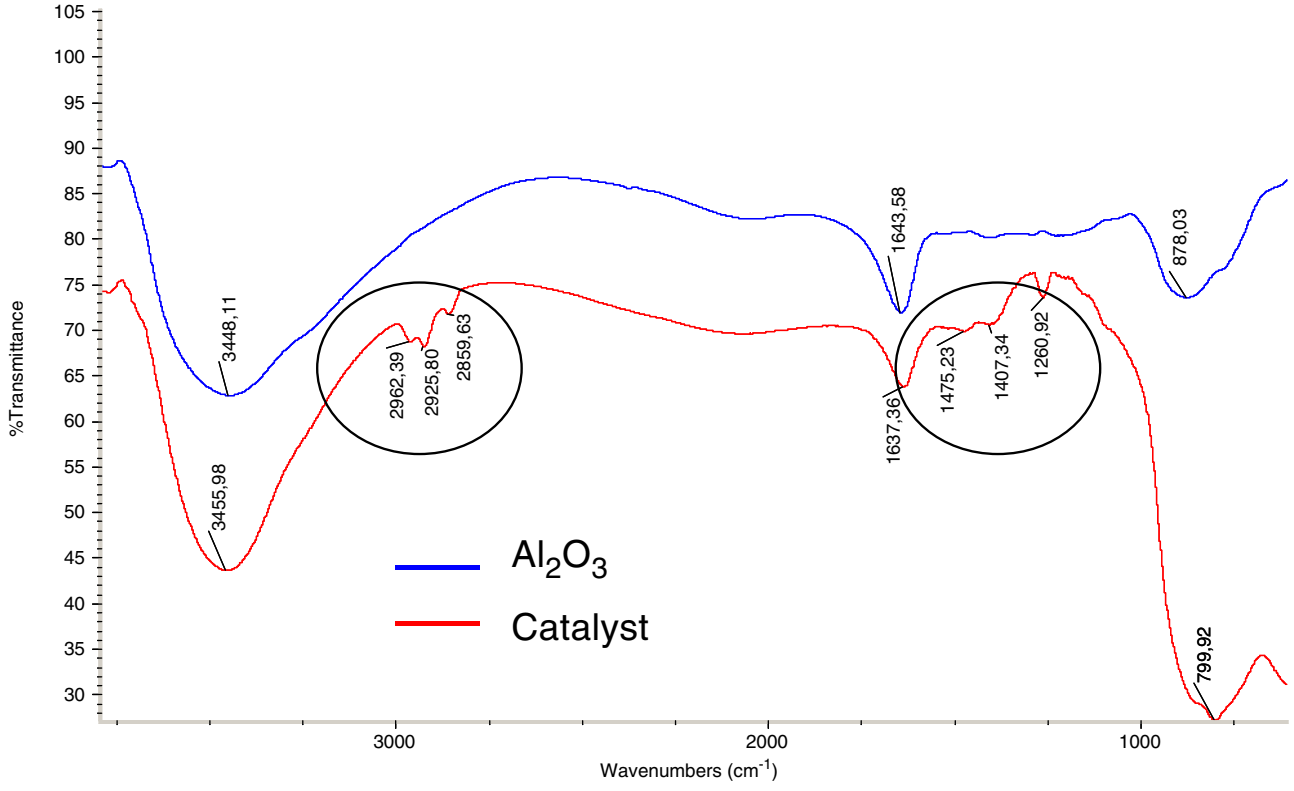

Fig. 5 EDAX of **a** Ni:Sn (2:1) and **b** Ni:Sn (3:1) in 2-methoxyethanol

Table 3 Electron diffraction pattern of NiSn–acetone particle

Dispersion	D (cm)	$d_{(h,k,l)exp}$ (Å)	Phase	$d_{(h,k,l)literature}$ (Å)
NiSn–acetone (2:1)	1.942	2.167	Ni (0, 0, 2)	2.172
	2.348	1.793	$NiSnO_3$ (0, 0, 0)	1.790
	3.275	1.285	Ni_3Sn_2 (2, 1, 1)	1.280
			Ni_4Sn (4, 0, 0)	1.280
			NiSn (14, 1, 2)	1.287
NiSn–acetone (1:2)	1.913	2.200	Ni_3Sn_4(−4, 0, 2)	2.200
	2.696	1.561	NiSn (3, 3, 1)	1.566
	3.304	1.274	NiSn (5, 1, 3)	1.274
			$NiSnO_3$ (0,0,0)	1.270
	4.203	1.001	Ni_3Sn (4, 1, 0)	1.001

267 nm. This fact can demonstrate the presence of different sizes from pure cluster or different clusters or alloys.

These values are consistent with that reported by Creighton and Eadon [27] for nanoparticles of 10 nm. The study of clustering phenomena is observed by the 207-nm peak. The spectra were recorded at different times (Fig. 2). Exponential decay of the maximum was observed as time passed. This behavior indicates that a fraction of the colloid coagulates and the other fraction remains stable in solution.

The particle size of different Ni–Sn bimetallic clusters is reliably summarized in Table 1, and micrographs for some representative systems and their respective histograms of relative frequency are seen in Figs. 3 and 4, respectively. Figure 3 shows the particle size of Ni–Sn–acetone (1:3) to be 14 nm. However, Ni–Sn–2-propanol (1:2) exhibits a particle size of 8 nm.

It is observed that for colloids with greater amounts of nickel, the size distribution of the monometallic Ni colloids agree with previous reports [25, 28]. Furthermore, if the amount of tin is increased, the size of particles is greater (~17 nm); this fact is well related to the stability since the Ni–Sn colloids in which there is a greater tin ratio are less stable than those with a greater amount of nickel.

The type of solvents represents an important issue; in the case of colloids prepared in 2-methoxyethanol, the distribution of size changes when the metallic ratio ranges between 6.7 and 10.5 nm. The same behavior is observed with 2-propanol that varies from 4.5 to 11 nm. However, in acetone and ethanol, the distribution of size is much wider, and it goes from a very small size of around 6 nm to a very great size such as 17 nm.

The energy dispersive X-ray analysis (EDAX) spectra in Fig. 5 allow us to corroborate the presence of the metals Ni and Sn; in addition to the elements that belong to the organic phase bound to metallic particles (C, H, O), they also they show the elements present in the grid (Cu and C) and impurities in the samples like silicon from silicone grease. It is possible to observe that the intensity of nickel proportion increases with the increase in its molar proportion in the bimetallic colloid.

In Table 3 the values obtained for some representative samples as well as the crystalline planes are transformed, which can justify the spacing found and obtained from the diffraction patterns shown in Figs. 6 and 7.

The analysis revealed the bimetallic particle presence of Ni–Sn in all the solvents, in addition to other phases, like for example SnO, SnO_4, Ni and Sn. The formed particles are mainly amorphous and are formed by very small crystallites that give very few diffraction rings, in which it is possible to observe crystalline material. In addition, it can be deduced that the crystallites are oriented in random form because if they were well oriented, instead of rings, they would appear as points.

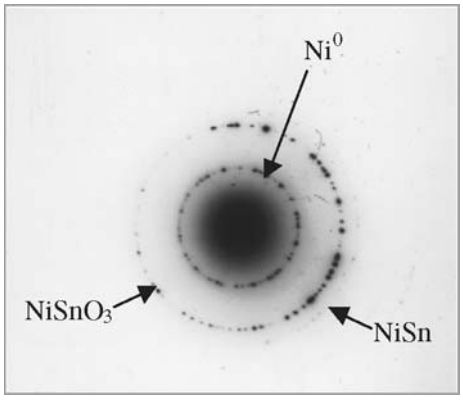

Fig. 6 Electron diffraction of NiSn–acetone colloids (2:1)

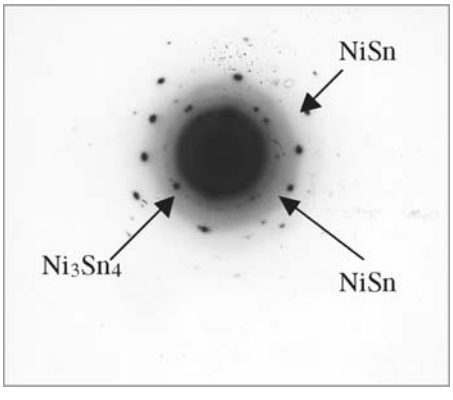

Fig. 7 Electron diffraction of NiSn–acetone colloids (1:2)

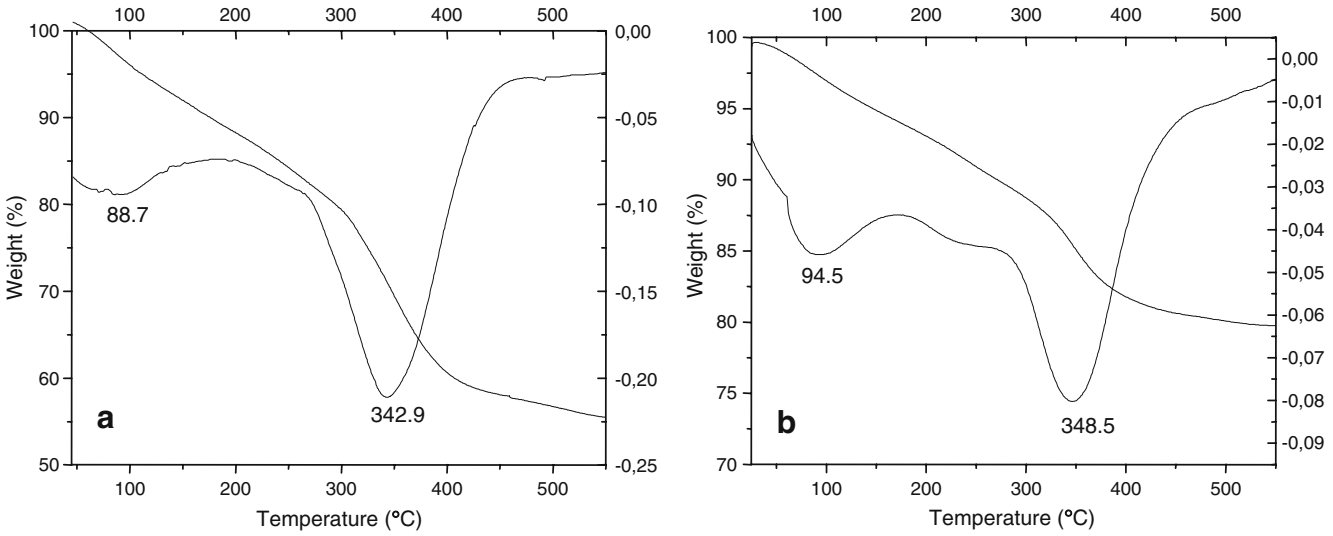

Fig. 8 Thermograms of **a** NiSn–2-methoxyethanol (2:1) and **b** NiSn–2-methoxyethanol (1:2)

The solids formed from the prepared colloidal dispersions exhibit a variable amount of reliability. The amount of incorporate reliability depends on the metal and reliability impelled [29, 30]. The thermograms for the Ni–Sn–2-methoxyethanol show that it is the most stable system (see Fig. 8).

The difference in thermal decomposition (TD) in thermograms of Ni–Sn–2-methoxyethanol (2:1) 342.9°C with respect to Ni–Sn–2-methoxyethanol (1:2) 348.5°C could be due to a greater preference and/or stability of the solvent towards the Sn surface. This is based on the fact that one phase has been significantly rich in tin surfaces for Pt–Sn and Ni–Sn systems [31].

Figure 9 shows the X-ray photoelectron spectra of the Ni 3p and Sn 3d of the Sn:Ni (3:1)–acetone solid. The binding energy (BE) of Ni $3p_{3/2}$ is 853.6–853.8 eV and that of Sn $3d_{5/2}$ is 484.6–487 eV [32].

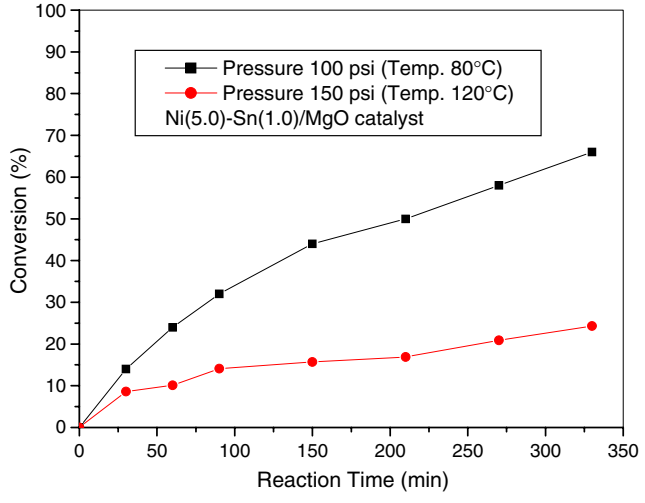

Fig. 9 **a** Ni 2p, and **b** Sn 3d core level spectra of NiSn(1:3)-acetone colloids

The BE of the Ni $3p_{3/2}$ peak is at approximately 853.2, corresponding to Ni^0 and Ni^{2+} species (the BE difference between two species is 0.8 eV). The curve fitting of the experiment spectra indicates reduced tin species, Sn^0 (484.6 eV) and oxides species (approximately 486.0 eV). Unfortunately, the state of the oxidized state, Sn^{2+} and Sn^{4+} cannot be distinguished by XPS [33].

The conductivity measurements were carried out for the Ni–Sn acetone solids. The study was performed to observe the influence of the metal percentage in the solids.

Electrical conductivity shows that the nickel is a metal, whereas tin is a semiconductor, and although in nanoparticles the electronic situation is different, the Sn stays like a semiconductor, whereas the nickel behaves from a conductor to an insulator.

It is possible to observe in Table 4 that Ni–Sn solids with greater amount of tin are in the rank of the semiconductors; however, in those with greater amount of nickel, they are insulating. This so abrupt change of behavior of nickel is possible due to the following reasons: the nickel easily oxidizes with the air, which means that this material offers

Table 4 Conductivity of NiSn–acetone films

Metallic powder	Ni:Sn	Electric conductivity (Ω^{-1} cm^{-1})	Particle size (nm)
Ni–acetone	1:0	1.2×10^{-7} (insulator)	5.9
Sn–acetone	0:1	9.4×10^{-2} (semiconductor)	15.7
NiSn–acetone	1:1	1.7×10^{-3} (semiconductor)	10.4
NiSn–acetone	2:1	2.9×10^{-5} (semiconductor)	8.60
NiSn–acetone	3:1	5.8×10^{-7} (insulator)	7.2
NiSn–acetone	1:2	7.5×10^{-2} (semiconductor)	14.1
NiSn–acetone	1:3	8.3×10^{-2} (semiconductor)	14.1

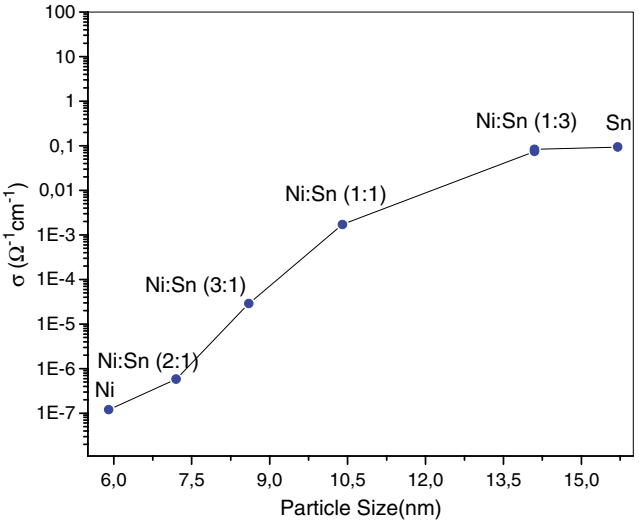

Fig. 10 Electric conductivity as a function of particle size

a greater resistance to the electrical current flow; the remaining solvent that is adhered on the surface of the material does not allow the contact between particles; the size of particles forming the solid is very small and, for that reason, exhibit a poor metallic character and carbonaceous species remains on the metallic surface, causing the increases in resistivity [34].

The solids that have greater amounts of tin display greater sizes of particles (see Table 4); therefore, when a high pressure is applied to the solid, a pellet is formed and a compact packing allows the contact among the particles (intra- and inter-particles linkage), increasing the transference. This electronic behavior is demonstrated in Fig. 10. In fact, it is possible to observe that as the size of particle increases, the conductivity is increased, behaving as insulating semiconductor systems e.g. Ni–Sn–acetone, $\sigma=5.8\times10^{-7}$ and Ni–Sn–acetone 1:3, $\sigma=8.3\times10^{-2}\ \Omega^{-1}\text{cm}^{-1}$.

All these systems show a paramagnetic behavior, following a simple Curie law, and they act like isolated systems (Fig. 11). It is observed that the increase in Ni in the relation of the Ni:Sn bimetallic ratio system (1:1, 2:1 and 3:1) causes an increase at the magnetic moment of the solid assets. On the other hand, the low magnetic moment presented for the Ni–acetone system (0.039 mB) could be attributed to impurities in the solid (O_2) and particle size. This diamagnetic contribution of the impurity causes a decrease in the measured value of the total magnetization with respect to the behavior displayed by Ni in the bulk state (0.606 mB), and the size of particles in the solid is very small where there is no contact between particles since they are more solvated, causing a low magnetization and the decrease in the magnetic moment [35].

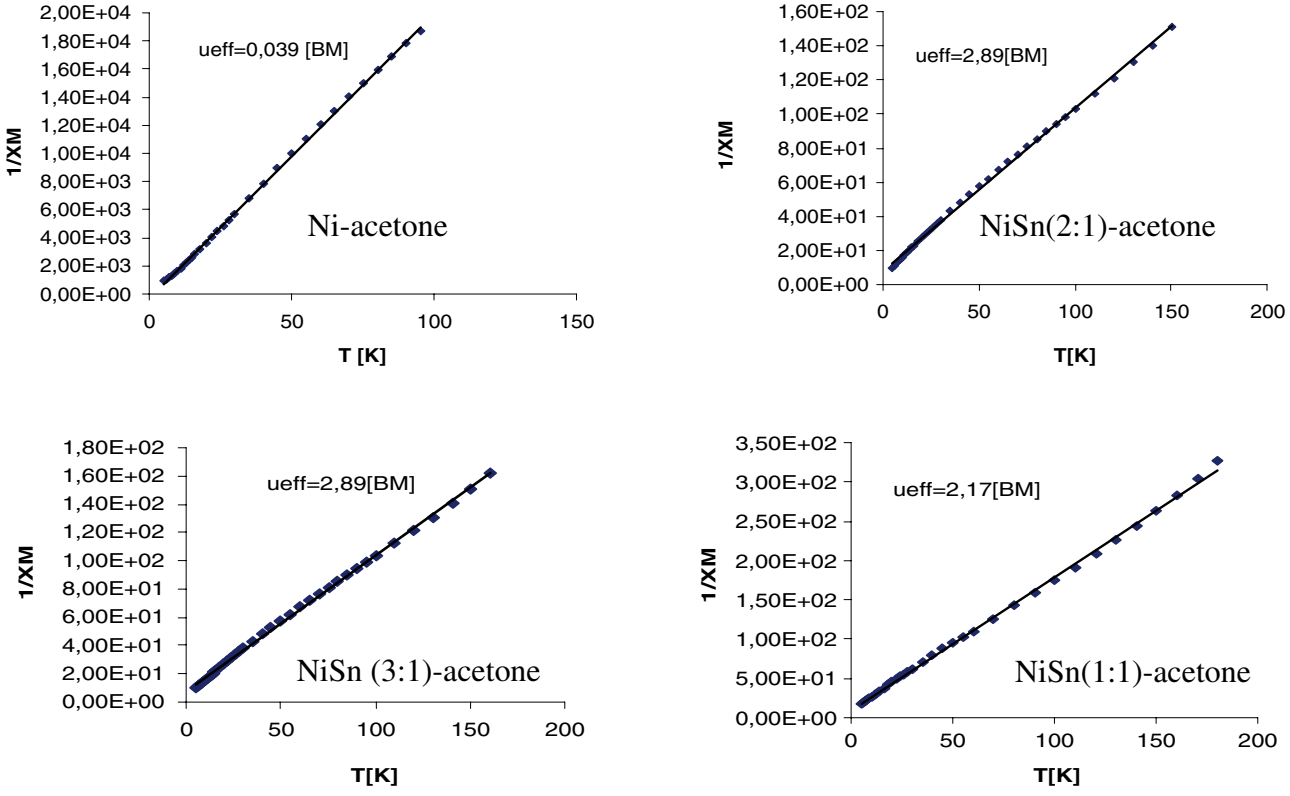

Fig. 11 Graphic inverse molar magnetic susceptibility (χM^{-1}) vs temperature (K) for Ni and NiSn acetone system

Conclusions

- The CLD synthesis of Ni–Sn gave as result colloids that are highly stable in 2-methoxyethanol and 2-propanol, and although a part of colloids of Ni–Sn flocculate quickly, another fraction remains in solution.
- The spectroscopic studies in the UV-Vis region revealed that the colloids of Ni continue absorption in the visible one, which is increased in region UV, with a band near 200 nm that corresponds to inter-bands transitions. A graphic representation became of the absorbance, and it was an exponential decay of the absorbance as a function of time.
- The colloids with greater percentage of Ni present positive charge, whereas the colloids with greater percentage of Sn have negative load. This must be due to an organic fragment adsorption that is in the surface of the metal.
- The study of the micrographs of colloids of Ni–Sn shows a distribution of size of particle between 5.9 and 17 nm. This distribution varies according to the reliability type and the Ni–Sn ratio.
- The EDAX corroborates the presence of the metals Ni and Sn. In addition, the intensity of nickel proportionally increases with the increase in its proportion to molar in the bimetallic colloid.
- By electron diffraction, the bimetallic particle determines Ni–Sn presence in all the solvents, in addition to other phases, like for example SnO, SnO_4, Ni and Sn.
- The solids with greater amount of Ni present display a greater loss of mass than those that have greater tin content. This is associated directly with the size of particle and the type of surface that presents these systems.
- It was determined that with an increase in the particle size, the conductivity increases, producing from insulating to semiconductor systems. This is indicative that a certain relation between the size and the form of cluster with the conductivity exists.
- All the systems present paramagnetism, and the low magnetic moment presented for the system Ni–acetone (0.039 mB) is attributed to impurities in the solid, like oxygen and particle size.
- By means of XPS, it was possible to determine that nickel can exhibit oxidation state 0 or 2+, and in the case of tin, the oxidation states 0 and higher (4+) are observed.

Acknowledgments The authors would like to acknowledge the financial support from FONDECYT (grant 1040456). Y. León acknowledges the scholarship from MECESUP. Dirección de Investigación and Laboratories from Facultad de Ciencias Químicas, Universidad de Concepción, Universidad de Concepción are acknowledged.

References

1. Schmid G (1992) Chem Rev 92:1709
2. Lewis LN (1993) Chem Rev 93:2693
3. Vokotin Y, Sinzing J, de Jong LJ, Schmid G, Vargaftik MN, Moiseev II (1996) Nature 384:621
4. Watzky MA, Finke RG (1997) J Am Chem Soc 119:10382
5. Roucoux A, Schulz J, Patin H (2002) Chem Rev 102:3757
6. Schmid G (1992) J Chem Soc Dalton Trans 1077
7. Frenkel A, Hills CW, Nuzzo RG (2001) J Phys Chem B 105:12689
8. Eason KA, Klabunde KJ, Sorensen CM, Handjipanayis GC (1994) Polyhedron 13:1197
9. Liu K, Nagodawithana K, Searson PC, Chien CL (1995) Phys Rev B 51:7381
10. Robinson AL (1976) Science 194:1150
11. Maught TH (1983) Science 220:1032
12. Gates BC (1995) Chem Rev 95:511
13. Richtsmeier SC, Parks EK, Liu K, Pobo LG, Riley SJ (1985) J Chem Phys 82:3659
14. Koltypin Y, Katabi G, Cao G, Prozorov R, Gedanken A (1996) Non-cryst Solids 201:159
15. Ely TO, Amiens C, Chaudret B, Snöck E, Verelst M, Raspaud M, Broto J (1999) Chem Mater 11:526
16. Koltypin Y, Fernandez A, Rojas TC, Campora J, Palma P, Prozorov R, Gedanken A (1999) Chem Mater 11:1331
17. Cárdenas G, León Y (2004) Colloid Polym Sci 282:394
18. Cárdenas G, Segura R (2000) Mater Res Bull 35:1369
19. Cárdenas G, González M, Salgado E, Morales J, Soto H (1999) Mater Res Bull 34:1911
20. Cárdenas G, Segura R, Morales J, Soto H, Lima CA (2000) Mater Res Bull 35:1369
21. Cárdenas G, Oliva R (1998) Mater Res Bull 33:1599
22. Cárdenas G (2005) J Chil Chem Soc 50:603
23. Cárdenas G, Oliva R (1999) Colloid Polym Sci 277:164
24. Booth F (1958) Prog Biophys Biophys Chem 3:131
25. Cárdenas G, Acuña J (2001) Colloid Polym Sci 279:442
26. Cárdenas G, Alvial M, Klabunde K J, Pantoja O, Soto H (1994) Colloid Polym Sci 272:310
27. Creighton J, Eadon D (1981) J Chem Soc Faraday Trans 87:3881
28. Cárdenas G, Tello A, Segura R (2001) Bol Soc Chil Quím 46:441
29. Klabunde KJ, Murdock T (1979) J Org Chem 44:3901
30. Cárdenas G, Oliva R (1996) Eur J Solid State Inorg Chem 33:1135
31. Skoog D, Leary J (1994) Instrumental analysis, 4th edn. Saunders, New York, p 662
32. Onda A, Komatsu T, Yashima T (2000) Phys Chem Chem Phys 2:2999
33. Nishiyama S, Hara T, Tsuruya S, Masai M (1999) J Phys Chem B 103:4431
34. Van Vlack L (1980) Engineer materials. Continental, Mexico, p 128
35. Ould T, Amiens C, Chaudret B (1999) Chem Mater 11:526